Revista Brasileira de Ciências Ambientais
Brazilian Journal of Environmental Sciences

Validated stoichiometric model for mineral phase quantification in commercial gypsums

Modelo estequiométrico validado para quantificação das fases minerais em gessos comerciais

Adriana Adrielle Lima Pinto[1], *Carlos Costa Dantas*[2], *Leonardo Bandeira dos Santos*[3], *Valdemir Alexandre dos Santos*[1]

ABSTRACT

Gypsum production is an energy-intensive process that contributes significantly to CO_2 emissions, particularly in regions that rely on biomass or fossil fuels for calcination. Improving mineralogical control is essential for reducing energy waste and enhancing the environmental performance of the gypsum industry. This study proposes and validates a stoichiometric model implemented in Python to estimate the proportions of dihydrate, hemihydrate, and anhydrite in commercial gypsums based on chemical composition and hydration water. The model was applied to natural gypsum ore and commercial casting and plastering gypsums from the Araripe Gypsum Cluster, Brazil's main production region. Differential thermogravimetric analysis (DTG) was used for validation, and strong agreement was observed between experimental and simulated results, with maximum deviations of approximately 2.11%. The findings demonstrate that accurate mineral phase estimation can support more precise control of calcination temperature and residence time. Consequently, the proposed model has the potential to contribute to reductions in specific fuel consumption, CO_2 emissions, and mineral waste generation when incorporated into industrial process-control strategies. The proposed approach provides a low-cost and scalable tool for environmental monitoring and decision support in gypsum production. The novelty of this work, in contrast to conventional analytical approaches, lies in the development and experimental validation of a stoichiometric computational model capable of estimating gypsum mineral phases from chemical composition and hydration water content. The Python implementation constitutes an accessible computational platform that enables rapid application of the proposed model in research and industrial environments.

Keywords: Gypsum calcination; Mineral phase quantification; Process control; Low-cost modeling; Setting time; Environmental monitoring.

RESUMO

A produção de gesso é um processo de alta demanda energética e relevante contribuição para as emissões de CO_2, especialmente em regiões que utilizam biomassa ou combustíveis fósseis na calcinação. O controle mineralógico adequado é fundamental para evitar desperdícios de energia e melhorar o desempenho ambiental do setor gesseiro. Neste estudo, propõe-se e valida-se um modelo estequiométrico implementado em Python para estimar as proporções de di-hidrato, hemidrato e anidrita em gessos comerciais, com base na composição química e no teor de água de hidratação. O modelo foi aplicado à gipsita natural e a gessos de fundição e revestimento do Polo Gesseiro do Araripe, principal região produtora do Brasil. A validação foi realizada por análise termogravimétrica diferencial (DTG), mostrando forte concordância entre resultados experimentais e simulados, com desvios máximos de aproximadamente 2,11%. Os resultados demonstram que a estimativa precisa das fases minerais pode subsidiar a otimização da temperatura e do tempo de residência nos fornos. Dessa forma, o modelo apresenta potencial para contribuir com a redução do consumo específico de combustível, das emissões de CO_2 e da geração de resíduos minerais quando empregado como ferramenta de apoio ao controle do processo industrial. A abordagem proposta constitui uma ferramenta de baixo custo e escalável para o monitoramento ambiental e o apoio à decisão na produção de gesso. A originalidade deste trabalho reside no desenvolvimento e validação experimental de um modelo computacional baseado em relações estequiométricas para estimativa das fases minerais em gessos comerciais. A implementação em Python constitui uma ferramenta para operacionalização do modelo, favorecendo sua aplicação rápida e reprodutível.

Palavras-chave: Calcinação da gipsita; Quantificação da fase mineral; Controle de processo; Modelagem de baixo custo; Tempo de pega; Monitoramento ambiental.

[1]Universidade Católica de Pernambuco – Recife (PE), Brazil.
[2]Universidade Federal de Pernambuco – Recife (PE), Brazil.
[3]Instituto Avançado de Tecnologia e Inovação – Recife (PE), Brazil.
Corresponding author: Adriana Adrielle Lima Pinto – Laboratório de Desenvolvimento de Novos Materiais da Escola de Tecnologia e Inovação da Universidade Católica de Pernambuco - Rua do Príncipe, 526, Boa Vista – CEP: 50050-385, Recife (PE), Brazil. E-mail: adrianaadriellelp@gmail.com
Received on: 12/15/2025. Accepted on: 07/07/2026.
https://doi.org/10.67790/rbciamb.026.2921

Introduction

Gypsum is a widely used construction material whose performance is strongly influenced by its mineralogical composition, particularly the relative proportions of dihydrate ($CaSO_4 \cdot 2H_2O$), hemihydrate ($CaSO_4 \cdot 0.5H_2O$), and anhydrite ($CaSO_4$). These phases are directly associated with calcination conditions, especially temperature and residence time, which govern dehydration reactions and, consequently, affect setting behavior, mechanical properties, and durability of gypsum-based products (Elert et al., 2023; Krejsová et al., 2024).

The calcination of gypsum rock is an energy-intensive process typically conducted at temperatures between 120 and 170 °C. Inefficient thermal control may lead to heterogeneous phase composition, increased fuel consumption, and the formation of undesirable phases, negatively affecting both product quality and process efficiency (Tang et al., 2019; Koper et al., 2020). In a broader context, mineral-based industries are recognized as significant contributors to global CO_2 emissions due to their reliance on thermal processes, reinforcing the need for improved process control and energy efficiency (Madlool et al., 2011; Andrew, 2018).

Accurate determination of mineral phase composition is therefore essential for both quality control and process optimization. Conventional analytical techniques, such as X-ray diffraction (XRD), thermogravimetric analysis (TG/DTG), and Fourier transform infrared spectroscopy (FTIR), provide reliable results but are often costly, time-consuming, and not easily accessible for routine industrial monitoring. This limitation highlights the need for alternative approaches that combine accuracy with operational simplicity.

Previous studies have demonstrated that mineral phase estimation can be approached through physicochemical modeling, particularly when supported by chemical composition data. However, most available methods rely heavily on instrumental analysis for validation and are not readily applicable in low-cost or real-time industrial contexts. In this study, differential thermogravimetric analysis (DTG) was adopted as a reference method due to its sensitivity to dehydration events and its ability to distinguish gypsum phases based on characteristic mass-loss profiles (Iwasaki and Koga, 2020).

The present work proposes a novel stoichiometric computational model for estimating mineral phase composition in commercial gypsums from chemical composition and hydration water content. The model was implemented in Python to provide an accessible, reproducible, and scalable computational environment, while the scientific contribution resides in the mathematical formulation and validation of the proposed stoichiometric framework.

Beyond its technical application, improved mineralogical control may contribute to enhanced process efficiency and reduced environmental impact. Since phase composition is directly linked to calcination conditions, improved mineralogical control may support better thermal control and potentially contribute to lower fuel consumption and reduced process inefficiencies. Such strategies are aligned with broader efforts toward energy optimization and emission reduction in mineral-based industries (Favier et al., 2018; Scrivener et al., 2018).

Therefore, this study aims to develop, validate, and assess the applicability of a low-cost stoichiometric model for mineral phase estimation in commercial gypsums, providing a practical tool for process control and supporting environmentally oriented optimization strategies.

Material and methods

Stoichiometric basis

The thermal conversion of gypsum rock ($CaSO_4 \cdot 2H_2O$) into hemihydrate ($CaSO_4 \cdot 0.5H_2O$) occurs through partial dehydration, as expressed in Equation 1 (Iwasaki and Koga, 2020):

$$2(CaSO_4 \cdot 2H_2O) + \text{heat} \rightarrow 2CaSO_4 \cdot 0.5H_2O + 3H_2O \quad (1)$$

The extent to which this reaction proceeds depends strongly on kiln temperature profiles, residence time, and thermal homogeneity, factors known to influence energy consumption and CO_2 emissions in the calcination process (Jiang et al., 2019; Bolson et al., 2025). Under higher temperatures or prolonged exposure, anhydrite ($CaSO_4$) may also form, following secondary reactions extensively documented in classical and contemporary studies (Badens et al., 1999; Shinya et al., 2016). These reactions were incorporated into the stoichiometric modeling framework given their relevance to both material performance and environmental efficiency, since deviations in phase composition may be associated with unnecessary thermal input and increased carbon footprint during calcination, as reported in previous studies.

Correction factor (CF)

Gypsum ore contains natural impurities (e.g., carbonates, oxides, and insoluble residues), which affect the effective CaO and SO_3 contents available for dehydration reactions. To account for these effects, a Correction Factor (CF) was introduced based on the difference in crystallization water between the natural gypsum and the corresponding commercial gypsum, as expressed in Equation 2.

$$CF = \frac{100 - (H_2O_{\text{Gypsum ore}} - H_2O_{\text{Calcined gypsum}})}{100} \quad (2)$$

where:

$H_2O_{\text{Gypsum ore}}$ is the water of crystallization content of the gypsum ore sample, determined by analytical methods.

$H_2O_{\text{Calcined gypsum}}$ is the water of crystallization content of the commercial gypsum sample.

This correction adjusts the stoichiometric balance by compensating for non-reactive phases present in the raw material, improving the accuracy of mineral phase estimation. From an environmental perspective, the CF also reflects process efficiency, since lower values may indi-

cate higher impurity levels, which can require additional thermal energy during calcination, thereby increasing fuel consumption and emissions (Bel-Anzué et al., 2017; Pedreño-Rojas et al., 2019).

Algebraic formulation for estimating the mineral phases in commercial gypsum

The mineralogical quantification model was structured from the stoichiometric relationship between available calcium oxide (CaO_{avail}) and SO_3. Three Primary Conditions (PC) were defined: (i) PC1, ideal stoichiometry; (ii) PC2, excess CaO; and (iii) PC3, excess SO_3. Each PC was further subdivided into Secondary Conditions (SC) according to the ratio between corrected oxides (CaO + SO_3) and hydration water. These SC groups—SC1 (hemihydrate predominance), SC2 (mixed system), and SC3 (dihydrate predominance)—allow classification of samples into combinations of dihydrate (D), hemihydrate (H), and anhydrite (A).

Table 1 summarizes the PC–SC relationships and respective algebraic expressions used for estimating mineral contents. Figure 1 presents the decision flowchart guiding the classification steps based on chemical composition (CaO, MgO, CO_2, SO_3) and thermogravimetric water content.

The formulation was designed not only for mineralogical accuracy but also to support environmentally efficient calcination, since accurate phase prediction may support better control of kiln temperatures and residence times, potentially contributing to reduced energy waste and CO_2 generation (Koper et al., 2020; Huang et al., 2024).

Computational implementation of the stoichiometric model

The proposed stoichiometric model was computationally implemented using the Python programming language (Mrabet and Sliti, 2024; Gohr et al., 2025), with the libraries Pandas, NumPy, and Matplotlib. The computational model:

- Calculates the CF,
- Determines Primary and Secondary Conditions,
- Applies the algebraic expressions corresponding to each PC–SC combination, and
- Outputs estimated percentages of D, H, and A phases.

To evaluate the tool's applicability to environmental process control, model outputs were compared with DTG experimental data, assessing accuracy and potential for use in optimizing calcination energy efficiency. Such computational approaches are increasingly recognized as enablers of low-carbon manufacturing and circular-economy strategies within mineral-processing industries (Chen et al., 2024).

The complete Python implementation of the proposed stoichiometric model is provided in the Appendix (Supplementary Code S1). The source code contains all computational routines required for CF calculation, determination of the primary and secondary conditions, mineral phase estimation, and generation of the final output, allowing full reproducibility of the proposed methodology.

Experimental characterization

The experimental characterization aimed not only to validate the mineralogical predictions of the stoichiometric model but also to assess how phase composition reflects environmental and operational efficiency in gypsum calcination. By linking DTG data and setting behavior to kiln performance, the study provides indicators that may be useful for interpreting process conditions associated with energy consumption, CO_2 emissions and process sustainability.

Mineral analysis by DTG

DTG was performed on seven commercial gypsum samples, including three casting gypsums (C1–C3) and four plastering gypsums (P1–P4). For each sample, six replicate analyses were conducted to ensure statistical reliability.

The thermograms displayed characteristic mass-loss peaks between 130 and 220 °C, corresponding to the sequential release of hydration water and directly associated with the proportions of dihydrate, hemihydrate, and anhydrite (Nascimento et al., 2025). The use of replicate measurements allowed the evaluation of data consistency and supported the validation of the proposed stoichiometric model.

Casting gypsums exhibited higher hemihydrate contents and minimal dihydrate, indicating controlled calcination with more uniform thermal exposure. In contrast, plastering gypsums showed significant amounts of anhydrite, suggesting prolonged residence times or higher kiln temperatures, conditions associated with increased energy demand and emissions (Elert et al., 2023).

Determination of setting times

The same set of samples (C1–C3 and P1–P4) was used for setting time determination, ensuring consistency between mineralogical characterization and physical performance evaluation. Initial and final setting times were measured in accordance with ABNT NBR 13207 (ABNT, 2017b) using the Vicat apparatus. Samples were prepared with 70 mL of water per 100 g of gypsum (ABNT, 2017a).

Casting gypsums presented shorter setting times (initial < 10 min; final < 20 min), consistent with their higher hemihydrate content and with calcination conditions that are generally associated with lower energy demand. Plastering gypsums exhibited longer setting times (initial 12–14 min; final > 30 min), reflecting their elevated anhydrite levels, which extend workability but also signal higher thermal exposure during manufacture.

These findings reinforce the relationship between mineralogy and process performance, suggesting that improved mineralogical control may contribute to reduced phase variability and may support strategies aimed at minimizing energy waste and environmental impacts.

Table 1 – Stoichiometric expressions for mineral phase quantification in commercial gypsums based on chemical composition and hydration water content

Primary condition	Secondary condition	Calculation expression
PC1 $CaO_{Avail}/SO_3 = 0.7 \pm \sigma_m$	**SC1** $(SO_3 + CaO_{Avail})/H_2O_{Gypsum} = 15.1 \pm \sigma_m$	$H = SO_3 + CaO_{Avail} + H_2O_{Gypsum}$
	SC2 $(SO_3 + CaO_{Avail})/H_2O_{Gypsum} > 15.1 + \sigma_m$	$H = 16.1 \cdot H_2O_{Gypsum}$ and $A = (SO_3 + CaO_{Avail} + H_2O_{Gypsum}) - 16.1 \cdot H_2O_{Gypsum}$
	SC3 $(SO_3 + CaO_{Avail})/H_2O_{Gypsum} < 15.1 - \sigma_m$	$D = [76.998 \cdot H_2O_{Gypsum} - 4.78(SO_3 + CaO_{Avail} + H_2O_{Gypsum})]/11.32$ and $H = SO_3 + CaO_{Avail} + H_2O_{Gypsum} - D$
PC2 $CaO_{Avail}/SO_3 > 0.7 + \sigma_m$	**SC1** $1.7 \cdot SO_3/H_2O_{Gypsum} = 15.1 \pm \sigma_m$	$H = 1.7 \cdot SO_3 + H_2O_{Gypsum}$
	SC2 $1.7 \cdot SO_3/H_2O_{Gypsum} > 15.1 + \sigma_m$	$H = 16.1 \cdot H_2O_{Gypsum}$ and $A = (SO_3 + CaO_{Avail} + H_2O_{Gypsum}) - 16.1 \cdot H_2O_{Gypsum}$
	SC3 $1.7 \cdot SO_3/H_2O_{Gypsum} < 15.1 - \sigma_m$	$D = [76.998 \cdot H_2O_{Gypsum} - 4.78(SO_3 + CaO_{Avail} + H_2O_{Gypsum})]/11.32$ and $H = SO_3 + CaO_{Avail} + H_2O_{Gypsum} - D$
PC3 $CaO_{Avail}/SO_3 < 0.7 - \sigma_m$	**SC1** $2.43 \cdot CaO_{Avail}/H_2O_{Gypsum} = 15.1 \pm \sigma_m$	$H = 2.43 \cdot CaO_{Avail} + H_2O_{Gypsum}$
	SC2 $2.43 \cdot CaO_{Avail}/H_2O_{Gypsum} > 15.1 + \sigma_m$	$H = 16.1 \cdot H_2O_{Gypsum}$ and $A = 2.43 \cdot CaO_{Avail} - 15.1 \cdot H_2O_{Gypsum}$
	SC3 $2.43 \cdot CaO_{Avail}/H_2O_{Gypsum} < 15.1 - \sigma_m$	$H = 2.43 \cdot CaO_{Avail} + H_2O_{Gypsum} - D$ and $D = [H_2O_{Gypsum} - (21.87/145 \cdot CaO_{Avail} + 9/145\ H_2O_{Gypsum})] \cdot 12470/1836$

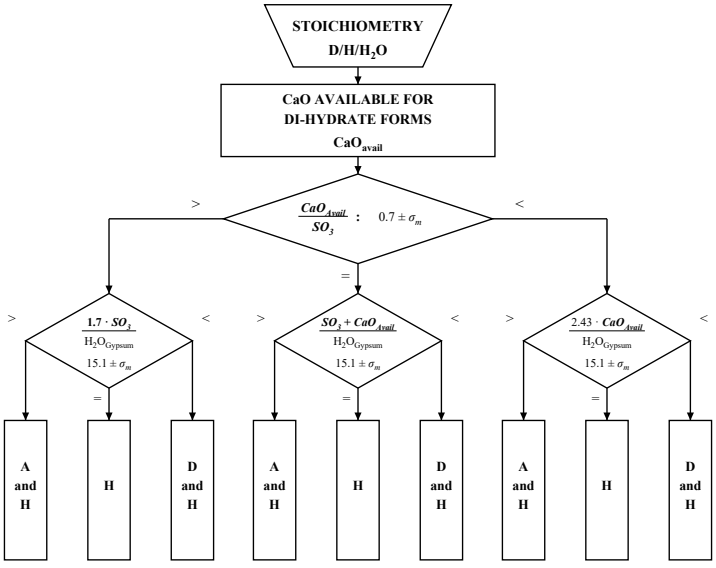

Figure 1 – Flowchart of the stoichiometric model for mineral phase estimation in commercial gypsums. The diagram presents the decision sequence based on chemical composition (CaO, SO_3, MgO, CO_2) and hydration water content, including classification into primary conditions (PC) and secondary conditions (SC), followed by the application of the corresponding algebraic expressions to estimate the proportions of dihydrate (D), hemihydrate (H), and anhydrite (A). Detailed equations are provided in Table 1 and in the main text

Results and discussion

Chemical and mineralogical characterization

The chemical composition of the gypsum rock used as raw material for the commercial gypsum samples analyzed in this study (Table 2) showed characteristics consistent with previous reports for high-purity materials from the Araripe Gypsum Cluster. The crystallization water content (~20%) is in agreement with the theoretical value for $CaSO_4 \cdot 2H_2O$, indicating the predominance of the dihydrate phase. Similarly, the CaO (32.50%) and SO_3 (45.23%) contents fall within the expected range for natural gypsum of high purity, as reported in both national and international studies (Hashemi et al., 2020).

Table 2 – Physicochemical analysis with average parameters of the gypsum mineral used in the development of this study

Determination	Quantification (%)
Moisture (45 °C)	0.07
Crystallization water (300 °C)	20.12
Loss on ignition (1000 °C)	1.32
Insoluble residues	0.30
Silica (SiO_2)	0.25
Iron and Aluminum (R_2O_3)	0.17
Calcium (CaO)	32.50
Magnesium (MgO)	0.14
Sulfur trioxide (SO_3)	45.23

The low contents of insoluble residues (0.30%), SiO_2 (0.25%), R_2O_3 (0.17%), and MgO (0.14%) further confirm the high purity of the material and suggest minimal interference from non-reactive mineral phases. These values are comparable to those observed in gypsum deposits with low impurity levels, supporting the classification of the raw material as suitable for efficient calcination processes.

It is important to note that the values presented in Table 2 correspond to the experimental physicochemical characterization of the natural gypsum rock used as feedstock for the commercial gypsum samples (casting and plastering) evaluated in this study. This ensures consistency between the raw material properties and the subsequent mineralogical and thermal analyses.

The DTG curve of the natural gypsum (Figure 2) exhibited a mass loss of approximately 20%, corresponding to the release of crystallization water, which is consistent with the expected behavior of $CaSO_4 \cdot 2H_2O$ during thermal decomposition (Iwasaki and Koga, 2020). This result further validates the chemical composition data and confirms the suitability of the material for use as a reference in the stoichiometric modeling approach.

Commercial gypsums displayed distinct dehydration patterns (Figure 3). Casting samples (C1–C3) were predominantly hemihydrate with minimal residual dihydrate, reflecting shorter and more uniform calcination, conditions typically associated with lower thermal energy demand. In contrast, plastering gypsums (P1–P4) contained significant anhydrite fractions, indicative of prolonged or higher-temperature calcination commonly used to extend workability. These differences were confirmed by the averaged mineral phase distributions (Figure 4), showing higher hemihydrate proportions in casting gypsums and increased anhydrite in plastering gypsums.

Setting times

Setting times measured using the Vicat apparatus (Figure 5), according to ABNT NBR 13207 (ABNT, 2017b), showed clear distinctions between product types. Casting gypsums (C1–C3) exhibited initial setting times between 9.0 and 9.2 min and final setting times

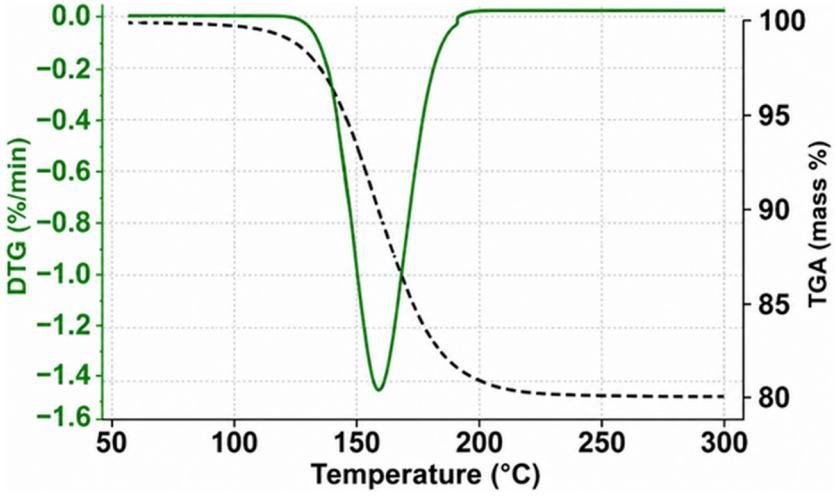

Figure 2 – Thermogravimetric (DTG) curve of natural gypsum rock. The profile shows a mass loss of approximately 20%, associated with the release of crystallization water, confirming the high purity and predominance of $CaSO_4 \cdot 2H_2O$ in the sample

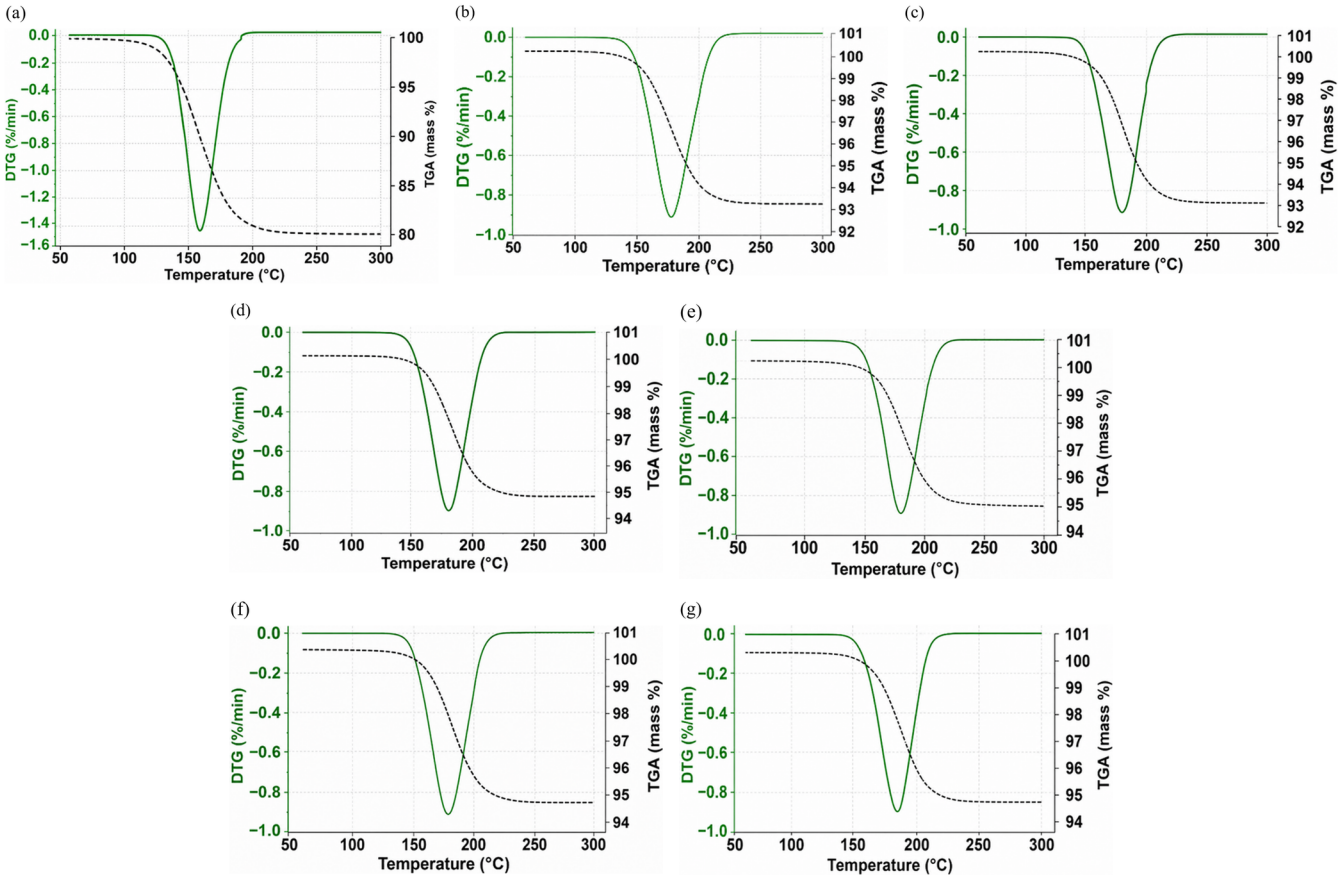

Figure 3 – DTG thermograms of commercial gypsums. (a–c) Casting gypsums (C1–C3); (d–g) plastering gypsums (P1–P4). The curves exhibit characteristic mass-loss peaks corresponding to dehydration reactions, indicating differences in mineral phase composition and thermal history between product types

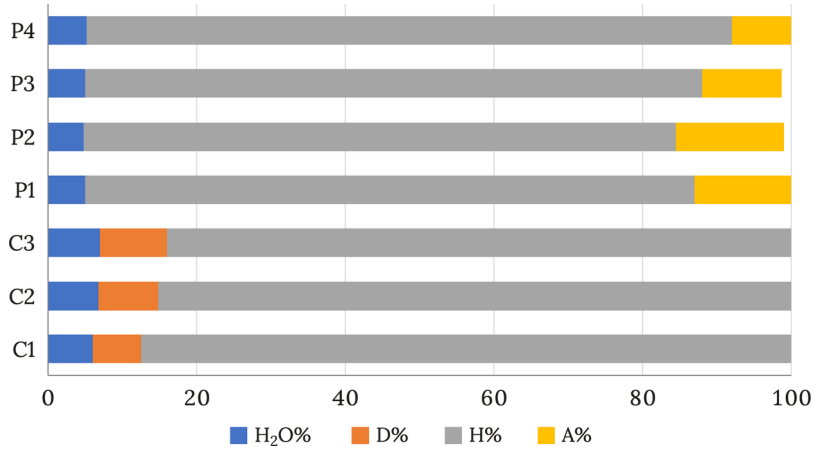

Figure 4 – Average mineral phase contents of casting and plastering gypsums. The results are expressed as percentages of dihydrate (D%), hemihydrate (H%), and anhydrite (A%). Casting gypsums (C1–C3) exhibit higher hemihydrate content, while plastering gypsums (P1–P4) show increased anhydrite fractions, reflecting differences in calcination conditions and thermal exposure

between 17.5 and 19.3 min, with workability times ranging from 8.5 to 10.1 min — values consistent with their higher hemihydrate content and with calcination conditions that avoid excessive thermal exposure. In contrast, plastering gypsums (P1–P4) presented longer initial setting times (11.8–14.3 min), final setting times (31.5–37.1 min), and workability times (19.5–24.2 min), consistent with elevated anhydrite contents and with the reduced solubility and slower hydration kinetics of this phase (Westgate et al., 2018; Iwasaki and Koga, 2020). Thus, the results quantitatively demonstrate the direct relationship between mineralogical composition, hydration behavior, and the thermal history of the material.

Comparison between experimental and simulated results

The proposed computational implementation of the stoichiometric model produced mineral phase estimates in excellent agreement with DTG measurements (Figure 6). Considering that the stoichiometric model is fully dependent on input chemical composition values, an uncertainty propagation analysis was performed to account for analytical errors in the input chemical composition. The resulting variability in predicted phase contents remained below 2.2%, reinforcing the reliability of the model.

In casting samples (C1–C3), differences in dihydrate (ΔD) and hemihydrate (ΔH) were below 2.2% (Table 3), confirming consistent calcination and strong model convergence. For plastering samples (P1–P4), the largest variations occurred in anhydrite (ΔA), but remained

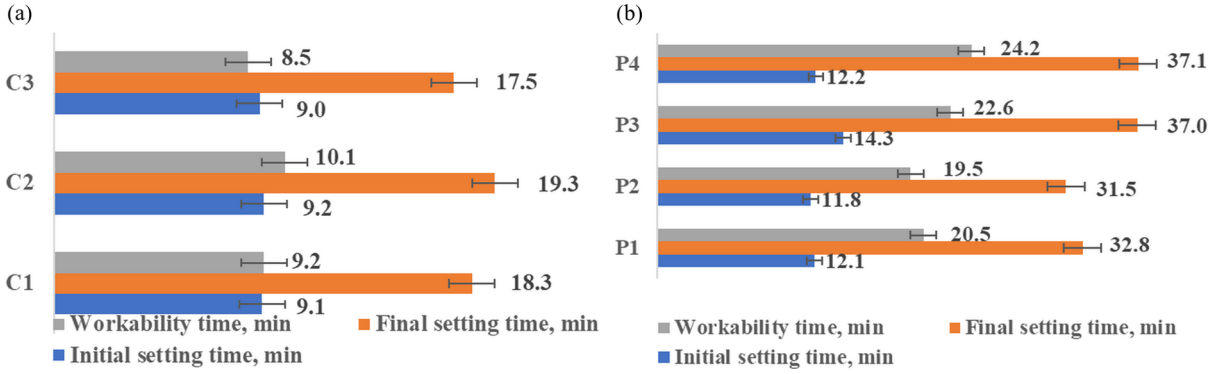

Figure 5 – Setting behavior of casting (C) and plastering (P) gypsums. (a) Initial and final setting times; (b) workability time. Values are expressed in minutes. Error bars represent standard deviation based on replicate measurements (n = 6 per sample). Casting gypsums (C1–C3) exhibit shorter setting times associated with higher hemihydrate content, whereas plastering gypsums (P1–P4) show extended setting and workability times due to increased anhydrite content

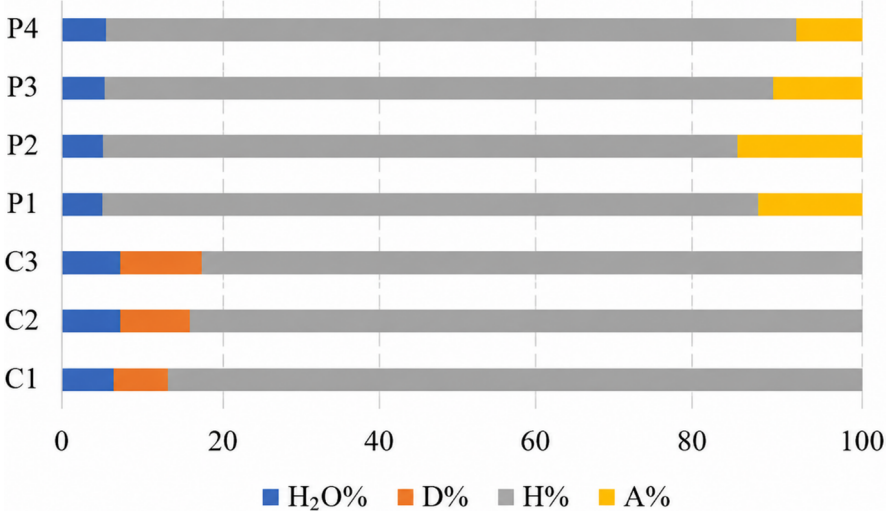

Figure 6 – Comparison between experimental (DTG) and simulated mineral phase contents obtained using the developed stoichiometric computational model. Results are shown for casting (C1–C3) and plastering (P1–P4) gypsums. The strong agreement between experimental and simulated values demonstrates the predictive capability of the proposed model for mineral phase estimation

within acceptable limits, reflecting the higher temperature sensitivity required for detecting this phase in DTG (Koper et al., 2020).

Low dihydrate contents in calcined samples indicate effective dehydration, modulated by kiln temperature and residence time (Krejsová et al., 2024). The presence of anhydrite in certain plastering products is consistent with extended thermal exposure, as observed in industry practices across the Araripe region (Koper et al., 2020).

Table 3 – Values of the differences between the percentage mineral contents determined by thermogravimetric analysis (DTG) and those obtained using the proposed stoichiometric model

Sample	ΔD (%)	ΔH (%)	ΔA (%)
C1	2.11	1.57	-
C2	1.72	1.67	-
C3	1.85	2.04	-
P1	-	1.32	2.03
P2	-	1.79	2.03
P3	-	1.34	1.84
P4	-	1.38	1.48

The differences between the mineral phase contents determined by DTG and those estimated using the proposed stoichiometric model were low, with a maximum absolute deviation of 2.11 percentage points (Table 3). To statistically evaluate the relationship between the experimental and simulated results, the coefficient of determination was calculated using the complete dataset, yielding an R^2 value of 0.9987. Figure 7 shows that the data points were closely distributed along the identity line, indicating strong agreement between the two methods. Together, the high coefficient of determination and the low deviations support the reliability of the proposed model for mineralogical estimation.

Environmental implications

The mineralogical information obtained from DTG analysis and the proposed algorithm-based stoichiometric model provides relevant insights into the environmental performance of gypsum production processes. Although this study does not directly quantify parameters such as fuel consumption or CO_2 emissions, it establishes a strong relationship between mineral phase composition and calcination conditions, which are known to influence energy efficiency and environmental impact.

The relative proportions of dihydrate, hemihydrate, and anhydrite are directly associated with kiln temperature and residence time. Therefore, accurate mineral phase estimation enables better control of these variables, which may contribute to process-control strategies intended to reduce overburning, lower fuel consumption, and improve material efficiency, as reported in previous studies (Pedreño-Rojas et al., 2019; Koper et al., 2020). These aspects are particularly relevant in the context of energy-intensive mineral industries, where process optimization is directly linked to emission reduction strategies and improved sustainability performance (Benhelal et al., 2013; Mikulčić et al., 2016).

From a broader environmental perspective, the optimization of calcination processes through improved mineralogical control aligns with global efforts to reduce carbon emissions in materials production, especially in sectors involving thermal treatment of mineral resources. Studies on cement and related materials have shown that even incremental improvements in process control can lead to significant reductions in energy consumption and greenhouse gas emissions (Madlool et al., 2011; Andrew, 2018).

In this context, the proposed model can be interpreted as a practical tool to support environmentally oriented process optimization,

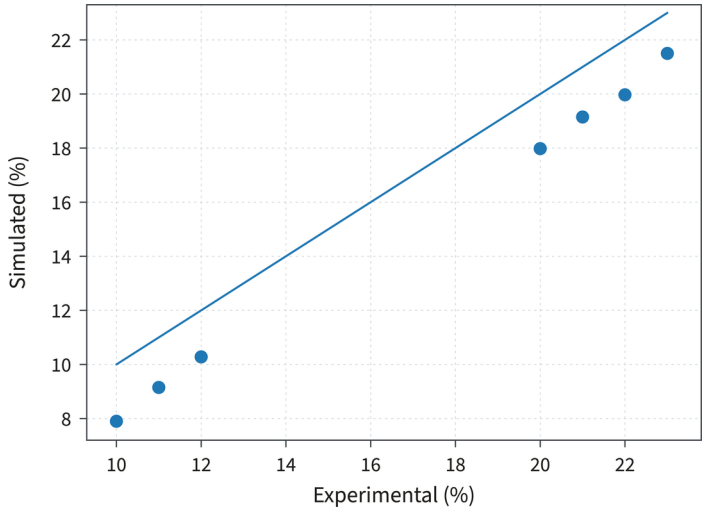

Figure 7 – Correlation between experimental (DTG) and simulated mineral phase contents (R^2 = 0.9987). The data points are closely distributed along the identity line (y = x), indicating excellent agreement and high predictive accuracy of the proposed stoichiometric model

contributing to improved efficiency and reduced environmental impact, particularly in small- and medium-scale production systems.

Conclusion

This study developed and experimentally validated a stoichiometric computational model for estimating mineral phases in commercial gypsums based on chemical composition and hydration water content. The computational implementation provides an efficient means for applying the proposed model, whereas the scientific contribution lies in the formulation and validation of the stoichiometric framework itself.

The results show that the proposed approach provides a reliable method for estimating the relative proportions of dihydrate, hemihydrate, and anhydrite, enabling improved interpretation of calcination conditions and their effects on material behavior. In this context, the model can serve as a low-cost complementary tool for mineralogical assessment and process control, particularly in industrial environments where access to advanced analytical techniques is limited. Because the mathematical framework is independent of the programming language employed, the proposed methodology can be implemented in different computational environments while preserving its predictive capability.

It should be noted that the model was developed and validated using high-purity gypsum materials, such as those from the Araripe Gypsum Cluster, and its performance is directly dependent on the accuracy of the input chemical data. Therefore, its direct application to more complex systems, including impure gypsums or phosphogypsum, may require calibration or extension of the stoichiometric framework to account for additional mineral phases and chemical constituents.

Although this study does not directly quantify environmental indicators such as energy consumption or CO_2 emissions, the results suggest that improved mineralogical control may support decision-making aimed at improving calcination efficiency under industrial operating conditions. In this sense, the proposed model has potential application as a decision-support tool for environmentally oriented process optimization. This perspective is consistent with broader efforts toward decarbonization in mineral-based industries, where improved process control and material efficiency are recognized as key strategies for reducing environmental impact (Lehne and Preston, 2018; Scrivener et al., 2018).

Future research should focus on validating the model under industrial operating conditions, integrating it into real-time monitoring systems, and expanding its applicability to a broader range of gypsum materials. Such developments may further enhance its usefulness as a practical tool for sustainable process management in the gypsum industry.

Authors' Contributions: Pinto, A.A.L.: conceptualization, data curation, formal analysis, methodology, writing; Dantas, C.C.: conceptualization, funding acquisition, supervision, writing; Santos, L.B.: data curation, formal analysis; conceptualization, funding acquisition, supervision, writing; Santos, V.A.: conceptualization, data curation, formal analysis, methodology, writing.

Conflicts of interest: the authors declare no conflicts of interest.

Funding: Coordination for the Improvement of Higher Education Personnel (CAPES: 88887.907687/2023-00) - National Council for Scientific and Technological Development (CNPq: 300938/2025-0) - Foundation for Science and Technology Support of the State of Pernambuco (FACEPE: BFP-0137-3.06/23).

Declaration on the use of generative artificial intelligence: During the preparation of this manuscript, ChatGPT (OpenAI) was used as a support tool for linguistic revision, structural organization, formatting, and readability improvement. After using this tool, the authors critically reviewed, edited, and validated all scientific content and take full responsibility for the final version of the manuscript.

References

Andrew, R.M., 2018. Global CO_2 emissions from cement production. Earth System Science Data, v. 10, 195–217. https://doi.org/10.5194/essd-10-195-2018

Associação Brasileira de Normas Técnicas (ABNT), 2017a. NBR 12128: gesso para construção civil – determinação das propriedades físicas da pasta de gesso. ABNT, Rio de Janeiro.

Associação Brasileira de Normas Técnicas (ABNT), 2017b. NBR 13207: gesso para construção civil – especificação. ABNT, Rio de Janeiro.

Badens, E.; Veesler, S.; Boistelle, R.; Chantain, D., 1999. Relation between Young's modulus of set plaster and complete wetting of grain boundaries by water. Colloids and Surfaces A: Physicochemical and Engineering Aspects, v. 156, 373–379.

Bel-Anzué, P.; Almagro, A.; Pérez, M.P.S.; Rodriguez-Navarro, S., 2017. Influence of the calcination process in traditional gypsum with structural behavior. Ge-conservación, n. 11, 79–85. https://doi.org/10.37558/gec.v11i0.456

Benhelal, E.; Zahedi, G.; Shamsaei, E.; Bahadori, A., 2013. Global strategies and potentials to curb CO_2 emissions in cement industry. Journal of Cleaner Production, v. 51, 142–161. https://doi.org/10.1016/j.jclepro.2012.10.049

Bolson, N.F.; Sarfraz, S.; Drewniok, M.; Basavaraj, A.; Hafez, H.; Purnell, P.; Salonitis, K.; Cullen, J., 2025. Assessing minimum energy requirements and emissions for different raw material compositions in clinker production. Environmental Research: Infrastructure and Sustainability, v. 5, 035005. https://doi.org/10.1088/2634-4505/adf146

Chen, L.; Yang, M.; Chen, Z.; Xie, Z.; Huang, L.; Osman, A.I.; Farghali, M.; Sandanayake, M.; Liu, E.; Ahn, Y.H.; Al-Muhtaseb, A.H.; Rooney, D.W.; Yap, P.S., 2024. Conversion of waste into sustainable construction materials: A review of recent developments and prospects. Materials Today Sustainability, v. 27, 100930. https://doi.org/10.1016/j.mtsust.2024.100930

Elert, K.; Bel-Anzué, P.; Burgos-Ruiz, M., 2023. Influence of calcination temperature on hydration behavior, strength, and weathering resistance of traditional gypsum plaster. Construction and Building Materials, v. 367, 130361. https://doi.org/10.1016/j.conbuildmat.2023.130361

Favier, A.; De Wolf, C.; Scrivener, K.; Habert, G., 2018. A sustainable future for the European cement and concrete industry. Cement and Concrete Research, v. 114, 119–128. https://doi.org/10.1016/j.cemconres.2017.08.022

Gohr, C.; Rodríguez, G.; Belomestnykh, S.; et al., 2025. Artificial intelligence in sustainable development research. Nature Sustainability, v. 8, 970–978. https://doi.org/10.1038/s41893-025-01598-6

Hashemi, M.; Saki, A.; Nikudel, M.R., 2020. Effects of chemical composition on the solubility and geomechanical characteristics of gypsum rocks from Gachsaran Formation, Iran. Bulletin of Engineering Geology and the Environment, v. 79 (7), 3785–3796. https://doi.org/10.1007/s10064-020-01794-y

Huang, Z.; Zhou, H.; Miao, Z.; Tang, H.; Lin, B.; Zhuang, W., 2024. Life-cycle carbon emissions (LCCE) of buildings: Implications, calculations, and reductions. Engineering, v. 35 (4), 120–146. https://doi.org/10.1016/j.eng.2023.08.019

Iwasaki, S.; Koga, N., 2020. Thermal dehydration of calcium sulfate dihydrate: Physico-geometrical kinetic modeling and influence of self-generated water vapor. Physical Chemistry Chemical Physics, v. 22 (39), 22436–22450. https://doi.org/10.1039/d0cp04195e

Jiang, B.; Xia, D.; Yu, B.; Xiong, R.; Ao, W.; Zhang, P.; Cong, L., 2019. An environment-friendly process for limestone calcination with CO_2 looping and recovery. Journal of Cleaner Production, v. 240, 118147. https://doi.org/10.1016/j.jclepro.2019.118147

Koper, A.; Prałat, K.; Ciemnicka, J.; Buczkowska, K., 2020. Influence of the calcination temperature of synthetic gypsum on the particle size distribution and setting time of modified building materials. Energies, v. 13, 5759. https://doi.org/10.3390/en13215759

Krejsová, J.; Kužel, R.; Keppert, M.; Scheinherrová, L.; Vimmrová, V., 2024. New insight into the phase changes of gypsum. Materials and Structures, v. 57, 128. https://doi.org/10.1617/s11527-024-02404-z

Lehne, J.; Preston, F., 2018. Making concrete change: innovation in low-carbon cement and concrete. Chatham House, London. https://doi.org/10.55317/9781784132729

Madlool, N.A.; Saidur, R.; Hossain, M.S.; Rahim, N.A., 2011. A critical review on energy use and savings in the cement industries. Renewable and Sustainable Energy Reviews, v. 15 (4), 2042–2060. https://doi.org/10.1016/j.rser.2011.01.005

Mikulčić, H.; Vujanović, M.; Duić, N., 2016. Reducing the CO_2 emissions in Croatian cement industry. Applied Energy, v. 164, 332–344. https://doi.org/10.1016/j.apenergy.2015.11.003

Mrabet, M.; Sliti, M., 2024. Integrating machine learning for the sustainable development of smart cities. Frontiers in Sustainable Cities, v. 6, 1449404. https://doi.org/10.3389/frsc.2024.1449404.

Nascimento, E.S.S.; Oliveira, H.A.; Santos, C.P.; Gomes, M.A.; Valerio, M.E.G.; Macedo, Z.S., 2025. Sustainable use of gypsum waste for applications in soil–cement bricks: mechanical, environmental, and durability performance. Ceramics, v. 8, 83. https://doi.org/10.3390/ceramics8030083

Pedreño-Rojas, M.A.; Flores-Colen, I.; Brito, J.; Liñán, C.R., 2019. Influence of the heating process on the use of gypsum wastes in plasters: mechanical, thermal and environmental analysis. Journal of Cleaner Production, v. 215, 444–454. https://doi.org/10.1016/j.jclepro.2019.01.053

Scrivener, K.L.; John, V.M.; Gartner, E.M., 2018. Eco-efficient cements: potentially economically viable solutions for a low-CO_2 cement-based materials industry. Cement and Concrete Research, v. 114, 2–26. https://doi.org/10.1016/j.cemconres.2018.03.015

Shinya, I.; Hiroaki, S.; Mikio, Y., 2016. Estimation of gypsum hemihydrate content in recycled gypsums derived from gypsum boards. Journal of Material Cycles and Waste Management, v. 18 (1), 168–176. https://doi.org/10.1007/s10163-014-0319-x

Tang, Y.; Gao, J.; Liu, C.; Chen, X.; Zhao, Y., 2019. Dehydration pathways of gypsum and the rehydration mechanism of soluble anhydrite γ-$CaSO_4$. ACS Omega, v. 4 (4), 7636–7642. https://doi.org/10.1021/acsomega.8b03476

Westgate, P.; Paine, K.; Ball, R.J., 2018. Physical and mechanical properties of plasters incorporating aerogel granules and polypropylene monofilament fibres. Construction and Building Materials, v. 158, 472–480. https://doi.org/10.1016/j.conbuildmat.2017.09.177

Appendix

Supplementary Code S1

```
# ---------------------------------------------------------
# CALCULATION OF MINERAL PHASES IN COMMERCIAL GYPSUM
# SUM OF MINERAL PHASES + SUM OF IMPURITIES = 100%
# ---------------------------------------------------------

# 1. IMPORT LIBRARY
import pandas as pd

# 2. GYPSUM ROCK DATA - INPUT DATA 1

MgO_content = 0.34        # MgO content in gypsum rock (%)
total_CO2 = 1.50          # Total CO2 content in gypsum rock (%)
total_CaO = 34.61         # Total CaO content in gypsum rock (%)
total_SO3 = 43.94         # Total SO3 content in gypsum rock (%)

# 2. HYDRATION WATER DATA – DATA INPUT 2
gypsum_water = 5.31       # Hydration water in commercial gypsum
  (%)
gypsum_rock_water = 20.12 # Water content in pure gypsum rock
  (%)
uncertainty = 0.02        # Maximum relative analytical
  uncertainty (2%)

# 3. MOLAR MASSES (g/mol) AND REFERENCE RATIOS
M_MgO = 40.30
M_MgCO3 = 84.31
M_CO2 = 44.01
M_CaCO3 = 100.09
M_CaO = 56.08
REFERENCE_PC_RATIO = 0.70
REFERENCE_SC_RATIO = 15.10

# 4. INPUT VALIDATION
input_contents = {
    "MgO_content": MgO_content,
    "total_CO2": total_CO2,
    "total_CaO": total_CaO,
    "total_SO3": total_SO3,
    "gypsum_water": gypsum_water,
    "gypsum_rock_water": gypsum_rock_water,
}

if any(value < 0 for value in input_contents.values()):
    raise ValueError("The reported contents cannot be
      negative.")
if gypsum_water == 0:
    raise ValueError("The hydration water content must be
      greater than zero.")
if not 0 <= uncertainty < 1:
    raise ValueError("Uncertainty must be entered as a fraction
      from 0 to 1.")

# 5. AVAILABLE CaO AFTER DEDUCTION OF IMPURITIES
# Step 1: MgO converted into equivalent MgCO3
calculated_MgCO3 = (MgO_content / M_MgO) * M_MgCO3

# Step 2: CO2 fraction associated with MgCO3
CO2_from_MgCO3 = calculated_MgCO3 * (M_CO2 / M_MgCO3)

# Step 3: remaining CO2 associated with CaCO3
remaining_CO2 = total_CO2 - CO2_from_MgCO3
if remaining_CO2 < 0:
    raise ValueError(
        "The CO2 calculated for MgCO3 exceeds the reported total
          CO2. "
        "Check the input data."
    )
calculated_CaCO3 = remaining_CO2 * (M_CaCO3 / M_CO2)

# Step 4: CaO associated with CaCO3
CaO_from_CaCO3 = calculated_CaCO3 * (M_CaO / M_CaCO3)

# Step 5: CaO available for sulfate phases
available_CaO = total_CaO - CaO_from_CaCO3
if available_CaO < 0:
    raise ValueError(
        "The CaO associated with CaCO3 exceeds the reported
          total CaO. "
        "Check the input data."
    )

# 6. CORRECTION FACTOR AND CORRECTED CONTENTS
correction_factor = (100 - (gypsum_rock_water - gypsum_water)) /
  100
if correction_factor <= 0:
    raise ValueError("The correction factor must be greater than
      zero.")

corrected_available_CaO = available_CaO / correction_factor
corrected_SO3 = total_SO3 / correction_factor
if corrected_SO3 == 0:
    raise ValueError("The corrected SO3 content must be greater
      than zero.")

# 7. PRIMARY CONDITION (PC)
pc_ratio = corrected_available_CaO / corrected_SO3
sigma_pc = REFERENCE_PC_RATIO * uncertainty
lower_pc_limit = REFERENCE_PC_RATIO - sigma_pc
upper_pc_limit = REFERENCE_PC_RATIO + sigma_pc

if lower_pc_limit <= pc_ratio <= upper_pc_limit:
    primary_condition = "PC1"
    oxide_sum = corrected_available_CaO + corrected_SO3
elif pc_ratio > upper_pc_limit:
    primary_condition = "PC2"
    oxide_sum = 1.70 * corrected_SO3
else:
    primary_condition = "PC3"
    oxide_sum = corrected_SO3

# 8. SECONDARY CONDITION (SC)
# SC3: below the interval – dihydrate and hemihydrate mixture.
# SC1: within the interval – hemihydrate.
# SC2: above the interval – hemihydrate and anhydrite mixture.
sc_ratio = oxide_sum / gypsum_water
sigma_m = REFERENCE_SC_RATIO * uncertainty
lower_sc_limit = REFERENCE_SC_RATIO - sigma_m
upper_sc_limit = REFERENCE_SC_RATIO + sigma_m

if sc_ratio < lower_sc_limit:
    secondary_condition = "SC3"
elif lower_sc_limit <= sc_ratio <= upper_sc_limit:
    secondary_condition = "SC1"
else:
    secondary_condition = "SC2"

# 9. MINERAL PHASE CALCULATION
hemihydrate = dihydrate = anhydrite = 0.0

if secondary_condition == "SC1":
    hemihydrate = (76.998 * gypsum_water - 4.78 * oxide_sum) /
      5.29
elif secondary_condition == "SC2":
    hemihydrate = 16.1 * gypsum_water
    anhydrite = oxide_sum + gypsum_water - hemihydrate
else:  # SC3
    dihydrate = (76.998 * gypsum_water - 4.78 * oxide_sum) /
      11.32
    hemihydrate = oxide_sum + gypsum_water - dihydrate

# Small negative values caused only by floating-point rounding
  are set to zero.
phases = {
    "Hemihydrate": hemihydrate,
    "Dihydrate": dihydrate,
    "Anhydrite": anhydrite,
}
for phase_name, value in phases.items():
    if value < -1e-9:
        raise ValueError(
            f"A negative content was obtained for {phase_name}
              ({value:.4f}%). "
            "Check the input data and model assumptions."
        )

hemihydrate = max(hemihydrate, 0.0)
dihydrate = max(dihydrate, 0.0)
anhydrite = max(anhydrite, 0.0)
mineral_phase_sum = hemihydrate + dihydrate + anhydrite
estimated_impurities = 100.0 - mineral_phase_sum

if estimated_impurities < -1e-9:
    raise ValueError(
```

```
        "The calculated mineral phase sum exceeds 100%. "
        "Check the input data and model assumptions."
    )

estimated_impurities = max(estimated_impurities, 0.0)
total_mass_balance = mineral_phase_sum + estimated_impurities

# 10. RESULTS TABLE
results = pd.DataFrame({
    "Parameter": [
        "Hydration water (%)",
        "Calculated MgCO3 (%)",
        "Calculated CaCO3 (%)",
        "Available CaO (%)",
        "Correction factor",
        "Corrected available CaO (%)",
        "Corrected SO3 (%)",
        "Lower PC limit",
        "PC ratio",
        "Upper PC limit",
        "Primary condition",
        "Oxide sum (%)",
        "Lower SC limit",
        "SC ratio",
        "Upper SC limit",
        "Secondary condition",
        "Hemihydrate, H (%)",
        "Dihydrate, D (%)",
        "Anhydrite, A (%)",
        "Mineral phase sum (%)",
        "Estimated impurities (%)",
        "Total mass balance (%)",
    ],
    "Value": [
        round(gypsum_water, 2),
        round(calculated_MgCO3, 2),
        round(calculated_CaCO3, 2),
        round(available_CaO, 2),
        round(correction_factor, 4),
        round(corrected_available_CaO, 2),
        round(corrected_SO3, 2),
        round(lower_pc_limit, 4),
        round(pc_ratio, 4),
        round(upper_pc_limit, 4),
        primary_condition,
        round(oxide_sum, 2),
        round(lower_sc_limit, 3),
        round(sc_ratio, 3),
        round(upper_sc_limit, 3),
        secondary_condition,
        round(hemihydrate, 2),
        round(dihydrate, 2),
        round(anhydrite, 2),
        round(mineral_phase_sum, 2),
        round(estimated_impurities, 2),
        round(total_mass_balance, 2),
    ],
})

# 11. DISPLAY RESULTS
print("\nRESULTS OF THE MINERAL PHASE ESTIMATION FOR COMMERCIAL
  GYPSUM:\n")
print(results.to_string(index=False))
```